Chapter 6

Optical Satellite Remote Sensing of the Coastal Zone Environment — An Overview

Ana C. Teodoro

Additional information is available at the end of the chapter

http://dx.doi.org/10.5772/61974

Abstract

Optical remote-sensing data are a powerful source of information for monitoring the coastal environment. Due to the high complexity of coastal environments, where different natural and anthropogenic phenomenon interact, the selection of the most appropriate sensor(s) is related to the applications required, and the different types of resolutions available (spatial, spectral, radiometric, and temporal) need to be considered. The development of specific techniques and tools based on the processing of optical satellite images makes possible the production of information useful for coastal environment management, without any destructive impacts. This chapter will highlight different subjects related to coastal environments: shoreline change detection, ocean color, water quality, river plumes, coral reef, alga bloom, bathymetry, wetland mapping, and coastal hazards/vulnerability. The main objective of this chapter is not an exhaustive description of the image processing methods/algorithms employed in coastal environmental studies, but focus in the range of applications available. Several limitations were identified. The major challenge still is to have remote-sensing techniques adopted as a routine tool in assessment of change in the coastal zone. Continuing research is required into the techniques employed for assessing change in the coastal environment.

Keywords: Shoreline Change Detection, Ocean Color, Optical Water Quality, River Plumes, Coral Reef, Alga Bloom, Bathymetry, Wetland Mapping, Hazards, Vulnerability

1. Introduction

One of the most useful reviews of remote sensing of the coastal zone was the work published by Cracknell [1], where a review of the current state of the use of remote sensing in estuaries and coastal waters at the end of the 20th century was performed. He identified that period (end of the 20th century) as a stage of potential great changes and advances in the use of remote sensing. Since then, the advances in the use of remote sensing for coastal areas have been huge. These advances are related to the availability of new sensors, more adequate for the study of this area, and also the improvements in the classification algorithms. Several useful reviews related to the value of remote sensing in the coastal zone environment have been published since then [2, 3]. Malthus and Mumby [2] update the information given by Cracknell [1], and highlight a number of priority areas. Advances were identified in the benefit of high spatial and spectral resolution data and complementary remote-sensing techniques. Further benefits are identified in rapid and more frequent data acquisition, faster and more automated processing and a greater sampling intensity over conventional field-based techniques. All these aspects were fully confirmed. Issues associated with adoption of remotely sensed data for coastal management were also discussed. This issue still is a topic of extreme importance. Although remotely sensed data are currently used for decision-making, their use is not yet an integrated tool for coastal management. Several research priorities were identified in the work of Malthus and Mumby [2]. Areas of value that continue to remain poorly investigated include the improvements to be gained from synergistic use of multiwavelength remote-sensing approaches, change detection techniques, and multitemporal comparisons and knowledge-based approaches to improve classification [2]. The lack of accuracy remains a challenge task. Therefore, the major challenge is to implement the remote-sensing techniques as a routine tool in assessment of coastal zone changes. Unfortunately, this challenge is still unfulfilled, as will be described in this chapter. More recently, Klemas [3] published an overview of remote sensing of emergent and submerged wetlands. Kelmas [3] discusses the impact of climate change on coastal wetland (sea-level rise, increase of temperature, and changes in precipitation), and the impacts due to anthropogenic activities. He has enumerated the recent advances in sensor design (high-resolution multispectral and hyperspectral imagers, light detection and ranging (LiDAR), and radar systems), and image processing techniques that making remote-sensing systems more practical and attractive for monitoring coastal ecosystems. The lack of accurate near-shore bathymetric data was identified as a key limitation in the application of geospatial data to coastal environments. He concludes that when remote-sensing systems are used wisely, including complementary combinations of different satellite and airborne sensors, they can provide data that enhance the research and management of coastal ecosystems. According to Klemas [3], the future research priorities should include better understanding and description of the radiative properties of coastal environments. Additional knowledge is required about the spatial and temporal variations of water column optical properties and its constituents. Best approaches for processing hyperspectral data need to be further investigated [3].

The main objectives of this chapter are (i) to provide an overview of the optical satellite remote sensing of the coastal zone environment and (ii) to highlight a number of application fields related to coastal areas where optical remote sensing plays an important role.

http://dx.doi.org/10.5772/61974

2. Optical remote sensing for coastal areas: Principles

Optical imaging sensors are a crucial technology in the field of coastal remote sensing. The main function of electro-optical imaging sensors is to collect incident electromagnetic (EM) radiation and convert it to a stored representation useful for remote-sensing analysis. These sensors operate in the optical region of the EM spectrum defined as radiation with wavelengths between 400 and 15000 nm. This range includes the visible (400–700 nm), the near infrared (NIR, 700–1100 nm), the short infrared (SWIR, 1100–2500 nm), the midwave infrared (MWIR, 2500–7500 nm) and the long-wave infrared (LWIR, 7500–15000 nm) spectral regions [4]. Optical remote sensing involves acquisition and analysis of optical data-EM radiation captured by the sensing modality after reflecting off an area of interest on ground/water. Different materials/ water constituents reflect and absorb differently at different wavelengths. Thus, the targets/ elements can be differentiated by their spectral reflectance signatures in the remotely sensed images. The optically active water constituents, including phytoplankton (chlorophyll a – Chla), detritus and minerals, Colored Dissolved Organic Matter (CDOM – also called gelbstoff or yellow substances), and water itself, all have an impact on the optical signature of water in the visible wavelengths. In the visible spectral range of solar radiation, light can penetrate in water bodies and its color can change due to scattering and absorption processes in the water body or at its bottom. This makes it possible to derive from optical remote-sensing data information about the characteristics of the water body and the type/concentration of its components. The water curve (spectral signature) is characterized by a high absorption at NIR wavelengths range and beyond. Because of this absorption property, water bodies as well as features containing water can easily be detected, located, and delineated with remote-sensing data. Turbid water has a higher reflectance in the visible region than clear water. This is also true for waters containing high Chla concentrations. Coastal waters are optically complex and the signal that a remote detector collects is a mixed signal including various water optically active constituents from different sources. Complex interaction among phytoplankton (Chla), Total Suspended Mater (TSM), and CDOM results in poor predictive ability in retrieval of various water quality proprieties in coastal waters.

Optical remote-sensing systems are classified into different types, depending on the number of spectral bands used in the imaging process: 1) Panchromatic imaging system: the sensor is a single-channel detector sensitive to radiation within a broad wavelength range. If the wavelength range coincides with the visible range, then the resulting image resembles a "black-and-white" image. 2) Multispectral imaging system: the sensor is a multichannel detector with a few spectral bands. Each channel is sensitive to radiation within a narrow wavelength band. The resulting image is a multilayer image which contains both the brightness and spectral information of the targets. 3) Hyperspectral Imaging Systems: the sensor acquires images in several (typically hundred or more) contiguous spectral bands. The precise spectral information contained in a hyperspectral image enables better characterization and identification of targets. Hyperspectral images have a great potential in applications regarding coastal management.

3. Sensors

In coastal and inland waters, optically active constituents often vary independently requiring improved spectral and radiometric resolutions, while physical drivers such as tides and geographic boundaries set up different spatial and temporal scales compared to the open ocean [5]. Due to the large number of sensors available, with distinct characteristics, it is a challenge to choose the most appropriate satellite images for monitoring coastal environments. The selection of the sensor is related to the applications required and the different types of resolution (spatial, spectral, radiometric, and temporal) should be considered. Another aspect that could interfere with the selection of the sensor is the data availability. Some images are really expensive and some data can be freely downloaded or granted by national/international organizations for research purposes. A list of the most relevant optical sensors used in the last decade to the assessment of coastal zone environment is shown in Table 1. A number of sensors have been launched since the Coastal Zone Color Scanner (CZCS) in 1978, including the Sea-viewing Wide Field-of-viewSensor (SeaWiFS), the MODerate resolution Imaging Spectroradiometer (MODIS), and the MEdium Resolution Imaging Spectrometer (MERIS). These instruments are equipped with sensors optimized for measuring water-leaving radiance or reflectance over most of the world's oceans, but not over many inland or coastal waters. Recently, significant advances have been made in studying coastal and inland waters using global sensors such as MODIS medium resolution data and MERIS full resolution (FR) data [6-8]. The primary mission of MERIS was the measurement of sea color in the oceans and in coastal areas. The applicability of MERIS data to coastal studies is extensive. Unfortunately, the MERIS instrument is no longer available (since May 2012).

Traditionally, the Landsat (TM and ETM+), the French Système Pour l'Observation de la Terre (SPOT), and Terra/ASTER have been reliable data sources for large coastal watersheds' land-cover [9, 10], water turbidity quantification [11], suspended sediments' concentration estimation [12-15], vegetation cover [16], among others. However, the 30 m, 20 m, and 15 m, respectively, spatial resolutions in the visible and Near Infra-Red (NIR) bands were initially designed for land-cover studies. The availability of high spatial and spectral resolution satellite data has significantly improved the capacity for mapping coastal ecosystems. High-resolution imagery obtained from satellites, such as IKONOS-2, Quick Bird-2, GeoEye-1, and Orbview-3 can be used for different purposes regarding coastal applications. WorldView-2 has a spatial resolution of 2 m for 8 multispectral (MS) bands (4 standard colors: red, blue, green, NIR, and 4 new colors: red edge, coastal, yellow, NIR2, and 0.5 m spatial resolution for the panchromatic (PAN) band (450–800 nm). The Pleiades 1A/1B satellites were designed with urgent tasking option, and images can be requested less than six hours before they are acquired. This functionality will prove invaluable in situations where the expedited collection of new image data is crucial, such as coastal crisis monitoring. This sensor is comparable to the other high-resolution sensors (e.g., GeoEye-1, Orbview-3). The Hyperion provides a high-resolution hyperspectral imager capable of resolving 220 spectral bands with a 30 m resolution. Through these spectral bands, complex coastal ecosystems can be imaged and accurately classified.

Sensor	Spectral Range (nm)	No. Bands	Spatial Resolution	Temporal Resolution	Swath width
Landsat TM	450–900 1550–2350 10410–12500	4 VNIR 2 SWIR 1 TIR	30 m 30 m 120 m	16 days	185 km
Landsat ETM+	450–900 1550–2350 10410–12500 520–900	4 VNIR 2 SWIR 1 TIR 1 PAN	30 m 30 m 60 m 15 m	16 days	183 km
SPOT 4-5 HRVIR	500–890 1580–1750 610–680	3 VNIR 1 SWIR 1 PAN	20 m 20 m 10 m	26 days	60 km
SPOT 5 HRS	500–890 1580–1750 510–730	3 VNIR 1 SWIR 1 PAN	10 m 20 m 5 m	26 days	60 km
ASTER	520–860 1600–2430 8125–11650	3 VNIR 6 SWIR 5 TIR	15 m 30 m 90 m	16 days	60 km
MODIS	620–14385	16 VNIR 4 SWIR 16 TIR	250 m–1 km	1 day	2330 km
SeaWIFS	402–885	8 VNIR	1.1 km	1 day	2800 km
MERIS	290–1040	15 VNIR	300 m	<3 days	1150 km
Hyperion EO-1	400–2500	220	30 m	16 days	8 km
IKONOS-2	455–850 760–850	4 VNIR 1 PAN	4 m 1 m	1–3 days	11 km
Quick Bird	430–918 405–1053	4 VNIR 1 PAN	2.44 m 0.61 m	<3 days	16.5 km
Orbview-3	450–900 450–900	4 VNIR 1 PAN	4m 1m	<3 days	8 km
GeoEye-1	450–920 450–800	4 VNIR 1 PAN	1.65 m 0.41 m	2.1–8.3 days	15.2 km
WorldView-2	400–1040 450–800	8 VNIR 1 PAN	1.85 m 0.46 m	1.1–2.7 days	16.4 km
Pleiades 1A/1B	430–950 480–830	4 VNIR 1 PAN	2.0 m 0.5 m	1 day	20 km
Sentinel-2	420–2370	VNIR-SWIR	10,20, 60 m	<3 days	290 km

Table 1. Characteristics of some optical systems used in coastal zones applications

Shortly, the assessment to the Sentinel-2 data will improve coastal environment monitoring programs. The Sentinel-2 was launched in June 2015 within COPERNICUS programme of the European Space Agency (ESA). The design of the Sentinel-2 mission aims at an operational multispectral Earth-observation system that complements the Landsat and SPOT and improves data availability for users. More information about Sentinel-2 can be found in Drusch et al. [17].

The development of specific techniques based on the processing of optical satellite data makes possible the production of information really useful for coastal environments, without any destructive impacts. Different image processing techniques have been applied to the satellite images in order to study the coastal environment. These techniques differ depending on the subject of study. Most of the techniques widely used in land and ocean studies are also applied in coastal research. Some techniques have also been intentionally developed to study specific aspects of this area. The topic of this chapter is not an exhaustive description of the image processing methods/algorithms employed in coastal environmental studies, but focus in the range of applications available. In this chapter will be gathered the most cited/important applications of optical remote sensing regarding the coastal zone environment of the last decade.

4. Applications

In this section, several application fields related to coastal environments, where optical remote sensing plays an important role, are addressed.

4.1. Shoreline change detection

Shorelines are inherently dynamic features that mark the transition between land and sea and are vulnerable to waves, winds, nearshore currents, and anthropogenic actions [18]. It is estimated that there are around 350 000 km of shoreline in the world and more than 60% of the world's population lives within 100 km of the coastal/sea. Therefore, monitoring and managing shorelines evolution are of considerable social, cultural, and economic importance. Furthermore, shoreline erosion and coastal flooding were highlighted among the gravest effects of climate change [19]. Several studies have investigated the potential of optical satellite images to study shoreline change. An idealized definition of shoreline is that it coincides with the physical interface of land and water [20]. Because of the dynamic nature of the idealized shoreline boundary, the use of shoreline indicators has been adopted for coastal studies. A shoreline indicator is a feature that is used as a proxy to represent the "true" shoreline position. Boak and Turner [21] reviewed shoreline definition and detection techniques, and carried out a comprehensive literature study. They categorized shoreline indicators in three groups: (i) visible discernible features; (ii) tidal datum-based indicators; and (iii) indicators based on the processing technique to extract the shoreline. One of the most common technique for shoreline detection was (and still is in some cases) visual interpretation. However, this approach is highly subjective and is not possible to access to any accuracy indicator. The alternative employs digital image processing techniques, as supervised and unsupervised classification algorithms. Gen [22] presents a paper that reviews the status of the use of remote sensing for the detection, extraction, and monitoring of coastlines. The review takes the US system as an example. However, the issues researched can be applied to any other part of the world. He concludes that visual interpretation of airborne remote-sensing data is still widely and popularly used for coastal delineation. However, a variety of remote-sensing data and techniques are available to detect, extract, and monitor the coastline.

Guariglia et al. [23] used a multisource approach to coastline mapping, in Basilicata region (Italy). They stated that satellite images are affected by tidal variations depending on their spatial resolution and concluded that the coastline can be extracted from Landsat TM images, without the interference of the tidal factor. Instead,tidal effects must be considered when the coastline is identified from images having higher spatial resolution that are comparable to the errors induced by tide.

Ekercin [24] present a work on the coastline movements at the northeast coasts of the Aegean Sea (Turkey). In this study, the coastline changes were examined using data from Landsat MSS, TM, and ETM collected between 1975 and 2001. In the image processing step, an unsupervised image classification algorithm (ISODATA) was employed and temporal image ratioing techniques were used to carry out coastline change assessment. Significant coastline movements were identified.

Maiti and Bhattacharya [25] used multidate satellite images from Landsat MSS, TM, ETM+, and ASTER to demarcate shoreline positions, from which shoreline change rates have been estimated using linear regression, along the coast of Bay of Bengal (India), between 1973 and 2003. The shorelines have been identified through the NIR bands, and included gray level thresholding and segmentation by edge enhancement technique. The result shows that 39% of transects have uncertainties in shoreline change rate estimations. On the other hand, 69% of transects exhibit lower Root Mean Square Error (RMSE) values for the short-term period, indicating better agreement between the estimated and satellite-based shoreline positions.

Kuleli et al. [26] presented a research focused on the shoreline change rate analysis by automatic image analysis techniques through histogram-based segmentation of land and water based on automatic thresholding algorithm, using multitemporal Landsat images (MSS, TM and ETM+) between 1972 and 2009 along the coastal Ramsar wetlands of Turkey. Accretion or erosion processes were observed on multitemporal satellite images along the areas of interest.

Kumar et al. [27] applied and developed the method established by Maiti and Bhattacharya [25] for calculating the rates of shoreline change, shoreline positions, and morphology of spits along the Karnataka coast, western India, for the period from 1910 to 2005 using multidated satellite images and topographic maps. Satellite images (IRS 1C, LISS-III) of IR band were employed. Binary images are used as input layers in unsupervised classification module to a complete separation between land and water classes, and to remove effect of suspended materials, if any. Significant changes in morphology of spits have been recorded.

Wang et al. [28] presented a class association rule algorithm on the basis of the Apriori algorithm. To test the feasibility of the method, Landsat ETM+ image scene of Jiaozhou Bay near Qingdao city (China) was used to interpret the coastline. First, the association rules of the sea–land separation of the study area were discovered from learning samples by using the class association rule algorithm. Second, the sea and the land of the image were separated with the mined rules. Third, the coastline was interpreted from the separation result. This approach includes not only spectral attributes but also the texture attributes (entropy) and the statistical analysis variables (mean and variance).

Regarding sand spits' behavior, Teodoro and Gonçalves [29] present different approaches in order to extract sand spits from IKONOS-2 data (Figure 1). A semiautomatic approach is proposed in this work, which is based on global thresholding through the Otsu's method, further refined through detected edges (GThE). The performance of GThE is compared with traditional pixel-based and object-based classification algorithms. The dataset is composed by six IKONOS-2 images, acquired between 2001 and 2007, covering a sand spit located in Portugal. The performance of the different methods used in the estimation of the sand spit area was evaluated through two sets of reference values of the sand spit area. The proposed GThE method presented better results than the other traditional methods, with a clear advantage of a considerable faster performance, beyond requiring a minimum operator intervention.

A high-precision geometric method for automated shoreline detection in the Spanish Mediterranean coast, from 45 Landsat TM and ETM+ imagery was presented by Pardo-Pascual et al. [30]. The methodology is based on an algorithm for subpixel shoreline extraction. The algorithm is based on the assumption that the separation between water and land will occur where the infrared intensity gradient around the pixel-level shoreline is maximum. The results confirm that the use of Landsat imagery for detection of instantaneous coastlines yields accuracy comparable to high-resolution techniques.

More recently, García-Rubio et al. [31] developed a method to identify the shoreline from satellite optical images (SPOT), applying an unsupervised classification (ISODATA), using the NIR spectral band to separate the sea and the land in Progreso (Yucatán, México). The shoreline was validated using quasi-simultaneous in situ shoreline measurements, both adjusted to equal water levels. The validation of shoreline obtained by satellite data revealed that the shoreline is located consistently seaward of the in situ shoreline. The success of this method suggests that it should be applicable to other locations, after adapting the confidence bounds to the beach conditions.

In conclusion, several techniques for coastline extraction and change detection from optical satellite imagery have been developed in the recent years. Manual identification, image enhancement, density slice using single or multiple bands, and image classification (supervised and unsupervised) are still the most common techniques employed. In addition, several image processing methods related to segmentation algorithms and statistics approaches have also been used. The data more used still are the traditional Landsat and SPOT images, but some works had also used high spatial resolution data (e.g., IKONOS 2), regarding the availability of an NIR band. In the future, should be considered the recent availability of the new sensors in conjunction with classification/segmentation algorithms more efficient. The

http://dx.doi.org/10.5772/61974

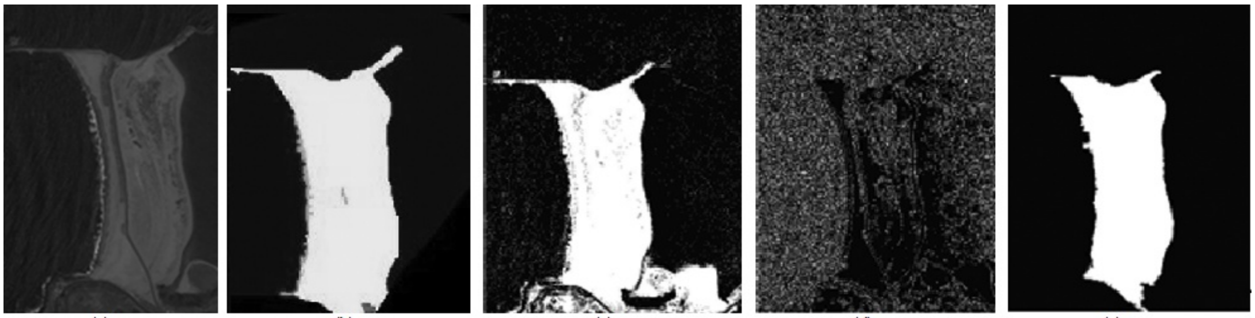

Figure 1. (a) Panchromatic band of the IKONOS-2 image from Jun. 2005; (b) the sand spit extraction with object-based approach; (c) global thresholding of the image in Fig. 1(a) through the Otsu's method; (d) edges of the image in Fig. 1(a) obtained through the Canny edge detector; (e) final extraction of the sand spit in Fig. 1(a), through the refinement of the global thresholding in (c) through the edges represented in (d) (adapted from [29])

accurate extraction of the shoreline is one of the most important parameter to estimate the erosion rates.

4.2. Coastal color

Remote sensing of ocean color has an important role to play as a cost-effective tool for global and frequent observations that can be interpreted in terms of surface concentrations of Chla, TSM, or CDOM. However, this global capability is to some extent questioned by the uneven distribution of field data that are at the basis of empirical algorithms, or are used for the definition of parameters in semianalytical bio-optical algorithms, and frequently these algorithms are not calibrated for coastal waters. The dominant optically active constituent in the open sea (case-1 waters) is the Chla, whereas in coastal waters (case-2 waters), TSM and CDOM often dominate the spectral signal of Chla [32].

Chlorophyll-a (Chla)

Chla is certainly the most commonly derived parameter in water quality mainly because of its use in determining the trophic status of waters. The Chla estimation allows forecasting of the phytoplankton concentration and is therefore an important component in the derivation of secondary products such as primary production. Several techniques/algorithms have been applied in order to estimate the Chla concentration [33]:

i. In high-biomass waters the 700/670 nm ratio reflectance has been widely used. The explanation for the strength of the correlation of Chla with the 700/670 nm is based on the interaction between backscattering from phytoplankton and the strong absorption of water, which both increase toward the IR. The offset to scattering due to absorption by water near 700 nm causes a sharp peak in highly scattering waters. The height and position of this peak is known to be well-correlated with Chla, with the peak shifting toward greater wavelengths (apx. 715 nm) as Chla increases. In contrast, the reflectance near 670 nm is uncorrelated, with Chla being almost constant owing to the Chla absorption maximum, which offsets backscattering. The positioning of the MERIS bands at 665 and 709 nm makes MERIS ideally suited for predicting

Chla using this ratio, and many studies have recently been carried out [34, 35]. Three-band algorithm has also been used to estimates of Chla in turbid and very high biomass hypertrophic waters [36]. A four-band algorithm, including an additional band near 700 nm, was found to be an improvement over the three-band model in highly turbid lake water through better accounting for absorption by water and nonnegligible scattering by TSM in the NIR band [37].

ii. The fluorescence maximum near 685 nm has been used to estimate Chla [38, 39]. The fluorescence line height (FLH) algorithm measures the height of the fluorescence peak at 685 nm from a linear baseline drawn between two points on either side of the peak [40]. It is important to consider that the FLH algorithm is only suitable for Chla concentrations generally not exceeding 30 mg m^{-3} as the backscattering peak near 700 nm overwhelms the fluorescence peak in high-biomass water.

iii. Sensors such as Landsat [41], SPOT [42], and IKONOS [43] are also frequently used to estimate Chla. However, the lack of narrow bands and low Signal–Noise Ratio (SNR) make very difficult the use of the algorithms already described. Therefore, simple linear regressions of single bands or band ratios are used and with less-significant correlations. An alternative could be the use of advanced algorithms, such as Artificial Neural Networks (ANN) and genetic algorithms [44], multivariate regression analysis [45], or spectral decomposition algorithm [46]. The use of these and other complex algorithms generally leads to improved significance of correlations.

Total Suspended Mater (TSM)

TSM is the total mass of suspended particles as measured per volume of water including inorganic (minerals) and organic (detritus and phytoplankton) components. The study of TSM concentration has a huge ecological importance, because the suspended matter is the main carrier of various inorganic and organic substances and becomes the main substrata for biochemical processes [47]. The TSM concentration affects ocean/coastal productivity, water quality, navigation, and coastal defense. The TSM concentration and distribution in the coastal zone varies with several hydrodynamic factors, such as tidal condition, currents' direction and velocity, river discharges, and wind stress [12]. The discrimination of TSM from water reflectance is based on the relationship between the scattering and absorption properties of water and its constituents. In the visible and NIR region, most of the scattering is caused by suspended sediments, and the absorption is controlled by Chla and CDOM. Therefore, the visible and NIR regions are the most adequate to estimate the TSM concentration. These absorptive in-water components decrease the reflectance in a substantial way. However, these absorptive effects occur generally for wavelengths less than 500 nm [32]. Several works have demonstrated that optical remotely sensed data can be used to retrieve TSM concentration from turbid coastal waters [14]. Many TSM models based on empirical methods have been used in operational satellite systems. These models were developed on the basis of statistical relationships between TSM concentrations and single-band or multiband reflectance [12, 13]. Although empirical models may be effectively applied to satellite images concurrent with the calibration dataset, their accuracy may be reduced outside the conditions of the calibration

http://dx.doi.org/10.5772/61974

dataset because of the empirical basis [48]. Therefore, semianalytical models that combine physical methods with statistical methods were proposed for several authors in order to retrieve the TSM concentration [49]. Teodoro et al. [12] present different methodologies to estimate the TSM concentration in a particular area of the Portuguese coast, from remotely sensed multispectral data (ASTER, SPOT HRVIR, and Landsat TM), based on single-band models, multiple regression, and ANNs. The analysis of the RMSE achieved by both the linear and nonlinear models supports the hypothesis that the relationship between the seawater reflectance and TSM concentration is clearly nonlinear. The ANNs have been shown to be useful in estimating the TSM concentration from reflectance of visible and NIR bands of ASTER, HRVIR (Figure 2), and TM sensors, with better results for ASTER and HRVIR sensors.

Colored Dissolved Organic Matter (CDOM)

CDOM, also called gelbstoff or yellow substances, is primarily composed of humic acids produced from the decomposition of plant litter and organically rich soils within coastal watersheds and upland areas is a significant contributor to water color, because humic substances absorb strongly in the blue region of the spectrum, turning the water brown. The absorption by CDOM (aCDOM – usually referenced at 440 nm) takes the form of an exponential function decreasing toward longer wavelengths so that its effects are usually negligible at wavelengths higher than 550 nm. CDOM concentrations increase in coastal waters due to the in situ creation of fulvic acids produced from the seaweed decomposition as a by-product of primary production estimulated by nutrients and the anthropogenic input of industrial or domestic effluents from populated areas. In the coastal environment, the optical properties of CDOM change owing to seawater mixing and photodegradation. Absorption by CDOM is one of the primary additive absorption Inherent Optical Properties (IOPs), along with phytoplankton and water, and is of great interest from a bio-optical perspective. Algorithms using ratios of reflectance in visible range have been found to be well-correlated with aCDOM [50]. In waters with low TSM concentration, Bowers et al. [51] showed theoretically, while making some assumptions about particulate absorption, that there is a linear relationship between aCDOM and the ratio of reflectance in the red and blue bands. Doxaran et al. [52] used a 400/600 nm ratio, whereas D'Sa and Miller [53] used the SeaWiFS band configurations 412/510, 443/510, and 510/555 nm, all of which gave good results, although this may reflect the existence of strong covariance between Chla and CDOM. Comparable red/blue ratios produced with the MERIS data also give similarly strong correlations [54]. The low radiometric resolution of some sensors (TM, IKONOS) makes CDOM estimations infeasible [55]. More recently, Loisel et al. [56] proposed a new method to assess aCDOM, based on the theoretical link between the vertical attenuation coefficient and the absorption coefficient. This method, confirmed from radiative transfer simulations and in situ measurements, and tested on an independent in situ data set allows aCDOM to be assessed with higher accuracy.

The optically active water constituents, including Chla, TSM, CDOM, and water itself, all have an impact on the optical signature of water in the visible wavelengths. The water-leaving radiance is modified through the backscattering and absorption of light by these constituents (IOPs). Absorption by Chla, CDOM and detritus, and water itself, are well-defined in the literature and can be used to explain the causal relationships between the observed remote-sensing reflectance and the biogeophysical parameters of interest. The backscattering coefficients for water, minerals, Chla, and TSM can be used in the same way. Strong absorption by water at wavelengths >750nm effectively masks out the signals from other constituents except in highly turbid water where scattering by minerals overwhelms absorption by water. Therefore, wavelengths between 400 and 750 nm generally contain the the most important information on the water constituents, which is detectable by remote-sensing instruments, with the exception of highly turbid water where the signal in the NIR is also useful [33]. Matthews [33] present a review of the empirical procedures of remote sensing in inland and near-coastal transitional waters. A review of empirical algorithms for quantitatively estimating a variety of parameters, including Chla, TSM, turbidity, and aCDOM, were proposed. The theoretical basis of the empirical algorithms was given using fundamental bio-optical theory of the IOPs. More recently, Mouw et al. [7] presented a review that describes the current and desired state of the aquatic satellite remote sensing, namely, mission capability, in situ observations, algorithm development, and operational capacity. They concluded that significant advances have been made in supporting in situ observations, algorithm development, and operational capacity and user engagement, but challenges still exist.

One of the major challenges in coastal and inland waters is the high turbidity and strong absorption. As absorption increases, the effect of self-shading of upwelling radiance increases. For IOPs, the available scattering sensors have the capability to effectively resolve backscattering at very high levels, but standard gain settings for these sensors are typically set to saturate at levels an order of magnitude lower to maximize resolution in the dynamic ranges observed in the ocean.

4.2.1. Optical Water Quality (OWQ)

Optical water quality (OWQ) has been defined by Kirk [57] as "the extent to which the suitability of water for its functional role in the biosphere or the human environment is determined by its optical properties." There are four main natural constituents, broadly classified, that attenuate light besides water itself: CDOM, TSM, nonalgal particulate organic matter (POM), and phytoplankton. Assessing OWQ involves quantifying the behavior of light in waters as affected by these light-attenuating constituents. Several publications have described the application of optical remote-sensing systems to measure water-quality conditions in lakes [45], river systems [58], and coastal zones [59, 60]. The interpretation of optical remote-sensing data of estuaries and tidal flat areas is hampered by optical complexity and often extreme turbidity. Extremely high concentrations of TSM, Chla and CDOM, local differences, seasonal and tidal variations, and resuspension are important factors influencing the optical properties in such areas [61].

There are mainly two approaches for deriving water-quality products from remotely sensed data: the model-based and the empirical approach. The model-based (or analytical) approach seeks to model the remote-sensing reflectance in terms of the water IOPs through radiative transfer modeling [62]. The remote-sensing reflectance from the water IOPs is obtained through a bio-optical model and an approximation of the radiative transfer equation [63] or through direct solution of the Radiative Transfer Equation (RTE). The reflectance at the top of the atmosphere can then be modeled using radiative transfer calculations for the atmosphere through codes such as 6S [64]. The main concerns with these kinds of algorithms are their sensitivity to errors from atmospheric correction procedures and the existence of nonunique or ambiguous solutions arising from the additive nature of the IOPs and the consequences of using a ratio in the reflectance approximation [65]. The analytical approach is complex and requires measurements of local/regional IOPs to develop a robust forward model. Empirical algorithms are relatively simple to derive and use: simultaneously acquired experimental sets of limnological, atmospheric, and remotely sensed data are used to normally derive site-and-time specific algorithms for a certain parameter using statistical regression techniques. These algorithms generally produce robust results for the areas and data sets from which they are derived. There are many varieties of algorithms that use either single bands, band ratios, band arithmetic, or multiple bands as independent variables in linear, multiple linear, or nonlinear regression analyses [33]. The empirical approach is computationally simpler, and it is employed in the majority of studies in inland waters.

Mélin and Vantrepotte [66] presented a study about the satellite data (SeaWiFS) available for coastal/shelf waters and marginal seas to derive a set of optical water types encompassing the full extent of the optical variability found in these regions. The spatial and temporal sampling considered is well-adapted to capture the optical variability found in coastal waters, whereas a higher level of averaging would tend to smooth out peculiar spectral characteristics. The focus of this work was all the coastal regions and marginal seas of the world. The classification allows the quantification of the optical similarity between regions. The set of 16 classes used in this work covers very turbid waters founded close to river outflow regions to oligotrophic waters. The general variability in optical types at any location has been addressed by quantifying the number of classes selected as dominant during the period and an index of optical diversity that has been linked to indices of marine biodiversity.

The works referred forecast an increasingly important role for OWQ studies driven by increased awareness of the need to protect ecosystems, manage water resources, and advance remote-sensing capabilities.

4.2.2. River plumes

River discharge into the coastal waters represents a major link between terrestrial and marine systems. River plumes are a mixture of freshwater and river sediment load, with some dilution caused by currents, and are affected by many factors such as river discharge, coastal wind fields, water stratification, surface layer mixing, tides and current, etc. It is known that plume waters near river mouths can contain high concentrations of nutrients and are excessively turbid [68].

CDOM is often used as an effective tracer for evaluating relative levels and the spatial distribution of dissolved organic carbon in aquatic environments. In addition, both Chla concentrations and turbidity are typically much higher in river systems, when compared to open sea environments. The river plumes are also distinguished from surround marine waters by their high concentration TSM, which changes the color of the ocean surface. Optical satellite images have been widely employed to study the spatio temporal variations of major river plumes around the world. The river plume observations/quantification included data from

AVHRR [69], SeaWiFS [70], MODIS [71], MERIS [72], Landsat TM/ETM [74], or combining data from different sensors [73].

Zhu and Yu [75] present a study that aimed to evaluate the effectiveness of an inversion algorithm for the extraction of riverine and estuarine CDOM properties at global scales through EO-1 Hyperion images applied to ten major rivers from five continents. The river plumes are distinguished from surrounding marine waters by their high concentration of TSM which changes the color of the ocean surface. Since the TSM concentration can be associated with nutrients, pollutants, and other materials, it is of crucial importance to remotely survey their dispersal in order to assess the coastal environmental quality of the regions surrounding river mouths.

Lihan et al. [76] present a study to identify the Tokachi River plume by satellite images (SeaWiFS) and determine its relationship with river discharge and clarify its temporal and spatial dynamics. A supervised (Maximum Likelihood – ML) classifier was used to identify the plume and empirical orthogonal functions were applied to determine the spatial and temporal variability of the plume during 1998–2002.

Gonçalves et al. [4] proposed an automatic procedure for the identification of the Douro river plume (Portugal) based on the thresholding of the 71 of MERIS FR scenes (level 2 data – TSM band) through an automatic search for the optimum value of the threshold parameter. A fully automatic method was considered and a comprehensive characterization of the river plume was performed through a set of attributes, which take into account not only the shape of the river plume, but also the TSM concentration values. Regarding the characterization in terms of shape, the following attributes were considered: size of the plume; corresponding to the number of pixels; perimeter; the major and the minor axis length of the ellipse adjusted to the river plume; and the orientation (Fig. 3).

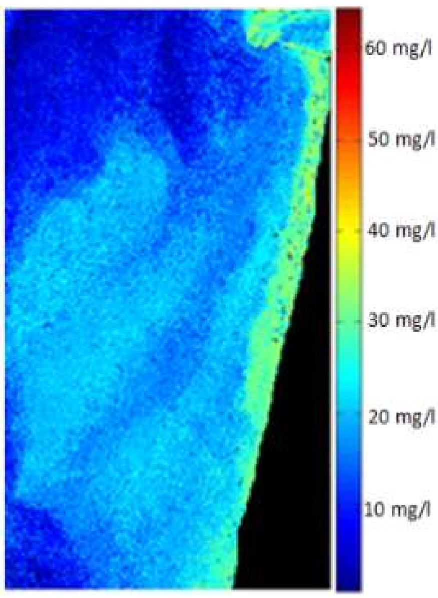

Figure 2. TSM concentration estimated from the HRVIR image through ANN for a region of the Portuguese coast

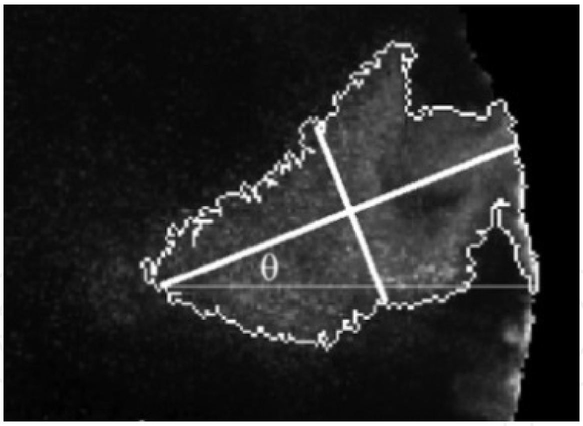

Figure 3. Illustration of the characterization of the river plume (2009-02-26) shape according to the adjusted ellipse (its major and minor axis) and the orientation of the river plume (adapted from [4])

Typically, outflow plumes are tracked in shelf water using density or salinity on account of the notably fresher composition of estuarine water. Unfortunately, there are no satellite-based remote-sensing platforms from which salinity can be directly measured. However, several studies have shown that these outflows carry large amounts of dissolved organic materials and suspended particles, which should allow plume events to be readily identified by remotely sensed optical images [77]. Kim et al. [78] related Chla concentration to salinity in the Changjiang plume area and presented the monthly summer plume area within a limited area during 1998–2007.

Hopkins et al. [79] used four satellite data products to examine the Sea Surface Temperature (SST), Sea Surface Salinity (SSS), Chla, and Mean Sea Level Anomaly (MSLA) fields in an area of the Angola Basin surrounding the Congo River mouth. Although it was not possible to extract a clear plume signature from the SST and MSLA alone, they provide useful supplementary understanding of the regions dynamics. Correlations between the SST, MSLA, Chla, and SSS help identify those areas persistently influenced by river input and those where variability is dominated by other processes.

4.2.3. Coral reef and Alga bloom

Coral reefs are one of the most biodiverse marine ecosystems on the planet. Worldwide, coral reef ecosystems are being increasingly threatened by sediment loads from river discharges, which in turn are influenced by changing rainfall patterns due to climate change and by growing human activity in their watersheds. Water turbidity and associated light attenuation are factors widely known to limit coral reef development. Coral reefs are generally limited to shallow and clear water with a mean water temperature of 18°C or higher, and are thus largely confined to the tropics [80]. Coral reef can be classified to show different forms of coral reef, dead coral, coral rubble, algal cover, sand, lagoons, different densities of seagrasses, etc. Several environmental variables have been shown to influence the biodiversity of a given habitat. Mapping such habitat variables could indicate the likely spatial distribution of biodiversity at a local scale and suggest priority areas for conservation, at least for the species for which habitat–biodiversity relationships have been identified. Remote-sensing technologies have been used to map coral reefs since the early days of Landsat program [81], and research into the use of remote-sensing technology continues with the advent of new sensors and data-processing methods [82]. The mapping of coral reefs and general bottom characteristics from satellites has become more accurate since high-resolution multispectral imagery became available [83, 84]. The development of hyperspectral instruments has also improved the degree to which accessory pigments can be used to separate detailed classes, and they have therefore enabled mapping of detailed classes while retaining satisfactory mapping accuracy [85, 86].

The work of Mumby et al. [85] reviews what can, might, and cannot be mapped using remote sensing, and not only covers aspects of reef structure and health but also discusses the diversity of physical environmental data such as temperature, winds, solar radiation, and water quality. Knudby et al. [87] reviewed coral reef biodiversity, the influence of habitat variables on its local spatial distribution, and the potential for remote sensing to produce maps of these habitat variables. Andréfouët et al. [88] present a review, where a new path is provided by following the diversity of units that have been mapped and characterized using high spatial resolution optical remote-sensing data for the main New Caledonian coral reef complexes and their individual reef-forming units. The combined examination of the different sources of data, and the exhaustive description of remotely sensed reef units, allows to a qualitative synoptic parallel to be drawn between the morphology of modern reefs and the contrasting patterns of reef growth, subsidence, and uplift rates occurring around New Caledonia. Hamel and Andréfouët [89] present a review about the use of very high resolution remote sensing for the management of coral reef fisheries. The rapid degradation of many reefs worldwide calls for more effective monitoring and predictions of the trajectories of coral reef habitats as they cross cycles of disturbance and recovery. Palandro et al. [90] used an 18-year (1984-2002) time series of Landsat 5/TM and 7/ETM+ images to assess changes in eight coral reef sites in the Florida Keys National Marine Sanctuary. A Mahalanobis distance classification was trained for four habitat classes. A detailed pixel-by-pixel examination of the spatial patterns across time suggests that the results range from ecologically plausible to unreliable due to spatial inconsistencies and/or improbable ecological successions.

Harmful Algal Blooms (HABs) phenomena are global and have been increasing in severity and extent, with many devastated implications. They cause eutrophic conditions, depleting oxygen levels needed for organic life, and limiting aquatic plant growth by reducing water transparency. HABs could be defined by an increase in the concentration of a phytoplankton species that has an adverse impact on the environment, with more serious implications when there is toxin production, but also with high biomass accumulation. HABs have been found to occur frequently in optically complex case-2 waters, such as in the Korean South Sea [91], East China Sea [92], Yellow Sea [91], Bohai Sea [93], Gulf of Mexico [94], among others. These blooms are dominated mostly by *Cochlodinium polykrikoides* (hereafter referred to as *C. polykrikoides*), *Alexandrium tamarense*, *Prorocentrum dentatum*, *Ceratium furca*, and *Karenia brevis*, causing massive mortalities of aquaculture fish and numerous ecological and health impacts since the last few decades. High concentrations of nutrients exported from agriculture

http://dx.doi.org/10.5772/61974

or urban sprawl in coastal watersheds are also causing algal blooms in many estuaries and coastal waters [95]. Satellite detection and monitoring of HABs require methods/algorithms that have been developed mostly based on extensive in situ bio-optical observations from optically less complex oceanic waters and optical modeling of water properties. Remote-sensing bio-optical algorithms explore the optical properties (absorption, backscattering, and reflectance) of each water component (CDOM, TSM, and Chla) in order to establish equations that can indicate a relationship between the optical characteristics of each component and the total sensor signals. These relationships are generally obtained through empirical, semianalytical, or radiation transfer models, and require in situ data in order to validate the equations/models. However, this approach is only appropriate for case 1 waters. Several spectral band algorithms have been developed to overcome the limitation of the standard optical algorithms. One of the most common methods for identifying a HAB is to estimate the Chla concentration. More details about the use of remote-sensing techniques for detecting phytoplankton and mapping HABs could be found in Klemas [95]. A range of disciplines including biochemistry, physical oceanography, and geology can be brought together to improve the identification of HABs.

4.3. Wetland mapping and coastal hazards/vulnerability

The coastal zone represents a comparatively small but highly productive and extremely diverse system, with a variety of ecosystems. Remote sensing allows to quantitatively retrieving several parameters useful for produce multi-hazard and vulnerability maps [96], wetland mapping [97] and identify infestations of invasive plants [98]. Satellite remote sensors can map coastal ecosystems and their changes cost-effectively at appropriate scales and resolutions, minimizing the need for extensive field and ship measurements. Traditionally, the Landsat TM and ETM and SPOT data have been reliable data sources for wetlands mapping [99]. The current status of methodologies and the most innovative works will be described in the following. The final part of this section will also include a brief reference to beach monitoring/classification, due to its importance in coastal management.

Wetland health is strongly impacted by runoff from land and its use within the same watershed. To study the impact of land runoff on estuarine and wetland ecosystems, a combination of models is frequently used, including watershed models, hydrodynamic models, and water-quality models [100]. The availability of high spatial and spectral resolution satellite data has significantly improved the capacity for mapping salt marshes and other coastal ecosystems [101]. Major plant species within a complex, heterogeneous tidal marsh have been classified using multitemporal, high-resolution images. Hyperspectral data have also been used for mapping coastal wetlands. The advantages and problems associated with hyperspectral mapping have been clearly demonstrated by Hirano et al. [102]. A number of techniques have been developed for mapping wetlands and even identifying wetland types and plant species [99, 103, 104]. To identify long-term trends and short-term variations, such as the impact of rising sea levels and hurricanes on wetlands, one needs to analyze time-series of remotely sensed imagery [105, 106]. Submerged aquatic vegetation is an important part of wetland and coastal ecosystems, playing a major role in the ecological functions of these habitats. Alga bloom and coral reefs have been discussed in section 3.3. The classification of Land Use and Land Cover (LULC) in delta regions was also the subject of several works. For instance, Fan et al. [107] investigated LULC in the Pear River Delta (China) using Landsat TM and ETM+ images and employed ML classifier. El-Kawy et al. [108] applied a supervised classification (ML) to four Landsat images (TM and ETM+) collected between 1984 and 2009 that provided recent and historical LULC conditions for the western Nile delta. The LULC mapping accuracy of 96% indicates that the integration of visual interpretation with the supervised classification of remote-sensing imagery is an effective method for the identification of changes in LULC. More recently, Tran et al. [109] presented a study where the main objective was to assess the spatiotemporal dynamics of LULC changes in the lower Mekong Delta (Vietnam) over the last 40 years. LULC change dynamics are derived from Landsat and SPOT satellite imagery between 1973 and 2011.

Vulnerability can be defined as the degree to which a person, community, or a system is likely to experience harm due to exposure to an external stress. Vulnerability also encompasses the idea of response and coping, since it is determined by the potential of a community to react and withstand a disaster [110]. A Multi-Hazard Vulnerability Map (MHVM) incorporates vulnerability in understanding the risk due to a hazard. Mahendra et al. [96] present a study that aims developing a methodology for assessing the multi-hazard vulnerability and gather quantitative estimate on the spatial extent of the inundation caused by composite hazards in Tamil Nadu state in the Bay of Bengal (India). The parameters used in this study were: shoreline change rate, sea level change rate, historical storm surges, and the high-resolution topography. Data from Landsat MSS, TM, and ETM and QuickBird were used to extract some parameters and, afterward, generate the hazard and risk maps. Risk maps and evacuation routes are generated by imbibing land use, transport, and structural information. Scientific study of the natural hazards and coastal processes of the Indian coast has assumed greater significance after the December 2004 tsunami because the country learned lessons on the impact of natural hazards in terms of high damage potential for life, property, and the environment. Several works were published related to this topic. Römer et al. [111] presents a case study that focuses on a local assessment of tsunami hazard and vulnerability, including the socioeconomic and ecological components. High-resolution optical data (IKONOS-2) were employed to create basic geo-data including LULC, to provide input data for the hazard and vulnerability assessment. Results show that the main potential of applying remote-sensing techniques and data derives from a synergistic combination with other types of data. Kumar et al. [27] develop a coastal vulnerability index for the maritime state of Orissa (India), using eight relative risk variables. Ortho-rectified Landsat MSS and TM images covering the Orissa coastline (India) for the years 1970, 1980, and 2000 were used to digitize the shoreline. Indian Remote Sensing Satellite (IRS) P6 Linear Imaging Self-scanning Sensor-IV (LISS-IV) was used to extract the coastal geomorphology. Zones of vulnerability to coastal natural hazards of different magnitude are identified.

Beach morphological classification was mainly based on in situ data (wave, tidal, and sediment parameters). However, parameters such as those are usually unavailable for several coastal areas. Optical remote sensing is a very powerful tool for beach monitoring/classification, since it allows identification and classification of beach morphologies. Teodoro et al. [112] applied a pixel-based (supervised or unsupervised) and region-based (object-oriented classification) classification to high-resolution data (aerial photographs and IKONOS-2 image) in order to identify, measure, and classify beach features/patterns and further classify the beach extension considered (Northwest coast of Portugal). Thereafter, in order to implement an automatic beach patterns extraction methodology, Teodoro et al. [113] present a new approach based on Principal Components Analysis and Histogram segmentation (PCAH) aiming to identify and analyze morphological features and hydrodynamic patterns, also applied to aerial photographs and IKONOS-2 image. More recently, Teodoro [114] applied data-mining techniques, particularly ANN and Decision Trees (DT), to the same image in order to identify and classify beach features and their geographic patterns. Teodoro [114] concludes that the use of ANNs and DTs for beach classification from optical remotely sensed data resulted in an increased classification accuracy when compared with traditional classification methods, as shown in Fig. 4. The results of this work should be used as an input in beach classification models, in sediment budget estimation, and also in the identification/characterization of rip currents and bars (location, spacing, persistence, size, and strength).

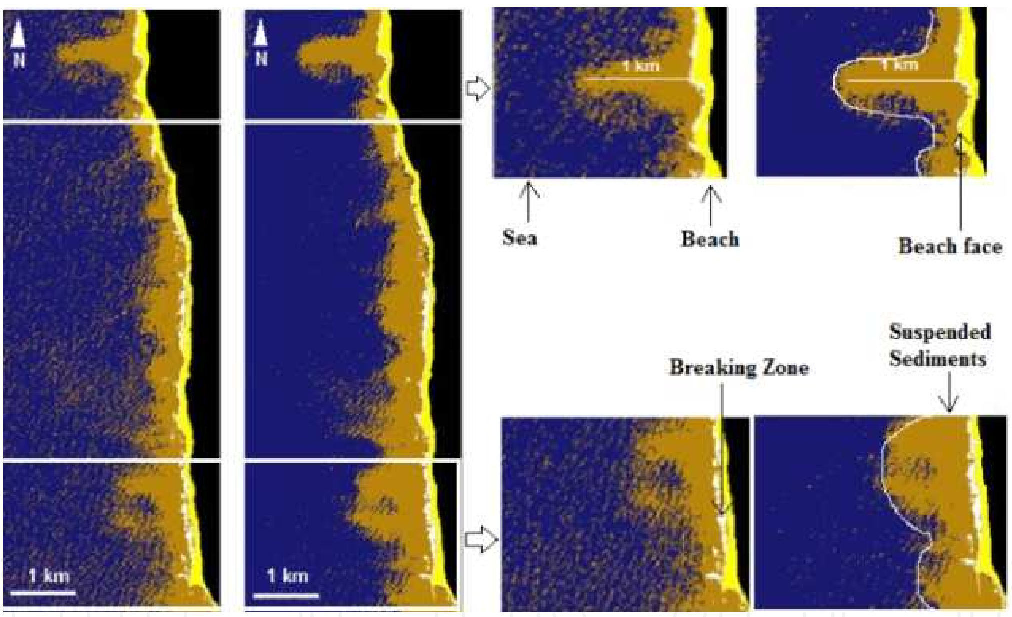

Figure 4. Beach patterns/forms identification and two zoomed areas obtained through (a) DT with pruning and (b) ANN (adapted from Teodoro [114])

Traditionally, the Landsat TM and ETM and SPOT satellite have been reliable data sources for wetlands mapping. However, in recent years the use of high spatial resolution data and hyperspectral data has become quite popular. In the vulnerability and hazards studies, different optical satellite data were commonly used to extract some parameters (e.g., shoreline change rate, land use) essential to hazard and risk maps generation. The use of high spatial resolution data is crucial. All these approaches are the key for a correct and efficient management of coastal environments.

4.4. Bathymetry

Bathymetric information is of crucial importance in coastal areas, such as in estuarine areas, which often exhibit a high population density, and vulnerable natural ecosystems. Optical remote sensing offers a cost-effective alternative to echo sounding and bathymetric LiDAR techniques for deriving bathymetric estimates in shallow coastal and inland waters [115- 117]. Images from optical remote sensors possess attractive properties for bathymetric mapping, including synoptic coverage of water surface areas, wide availability for most geographical regions, and relatively low cost [118]. The availability of optical high-resolution satellites, such as IKONOS, QuickBird, and WorldView, has renewed interest in applying optical remote-sensing techniques to the retrieval of bathymetric information for shallow coastal and inland waters, due to their high spatial resolution and enhanced water penetration capability. In this context, several inversion algorithms and models have been proposed in the literature for retrieving bottom depth estimates from multispectral remote-sensing imagery [115, 116, 118-120]. The simplest method of retrieving water depth from single-band remote-sensing imagery was first proposed by Lyzenga [121]. Later, Lyzenga [122, 123] derived a log-linear inversion model for inverting multispectral imagery to water depth. This inversion model uses the linear logarithmic-transformed multispectral remote-sensing data as the predictors to estimate water depth.

Minghelli-Roman et al. [124] present a comparison of bathymetric estimation using different satellite images (Quickbird, ETM, Hyperion, MERIS) in coastal seawaters. The aim of this study was to compare, for one bathymetric estimation method and one mesotrophic site, the results of depth estimation with a large panel of satellite and aerial images. For each image, the pair of spectral bands chosen to compute the bathymetry has been optimized. This comparison was discussed, in order to identify the influence of image parameters (spectral bands, SNR, spatial resolution, and quantization) on the bathymetric results and to propose the most adapted image parameters for bathymetric estimation. Regarding the depth RMSE errors obtained, no sensor seems to be the perfect sensor to estimate bathymetry. Regarding the spectral configuration, three spectral bands are required to generate the mask on water: the first in the blue-green domain; the second in the green domain; and a final band in the near-infrared domain. The atmospheric correction has to be efficient because a strong diffusion operates in the blue domain. A very high resolution such as Quickbird's is not necessary, but a lower resolution than 30 m induces mixed pixels on the shore and then degrades the estimation in shallow waters.

Teodoro et al. [125] propose a model for the estimation of depth based on Principal Component Analysis (PCA) of an IKONOS-2 image, for the Douro River estuary (Porto, Portugal). Subsequently, Teodoro et al. [117] proposed alternative univariate and bivariate models for the same IKONOS-2 image based on PCA and Independent Component Analysis (ICA). The PCA is the standard method for separating mixed signals. Such analysis provides signals that are linearly uncorrelated. Although the separated signals are uncorrelated they could still be depended, i.e., nonlinear correlation remains. The ICA was developed to investigate such data. The results obtained were compared with the bathymetric estimation through PCA. Best univariate ICA-based model allowed to estimate depth with a mean error that outperforming the best PCA based univariate model results, even with the first PCA component explains 80% of data variance. With bivariate models the results improved.

http://dx.doi.org/10.5772/61974

Kanno et al. [116] proposed a method that combines a spatial interpolation method based on nonparametric regression and Lyzenga et al. [115] method on a statistical basis. A multispectral image of QuickBird of a coral reef site along Ishigaki City (Japan) was used in this approach. This method is based on a semiparametric regression model that consists of a parametric imagery-based term and a nonparametric spatial interpolation term that complement one another. An accuracy comparison in a test site showed that this new method is more accurate than either of the existing methods when sufficient training data are available and far more accurate than the spatial interpolation method when the training data are scarce.

Su et al. [118] propose a geographically adaptive inversion model for improving bathymetric retrieval in complex and heterogeneous marine environments for Hawaiian Islands. By using IKONOS-2 and Landsat ETM+ images, they demonstrated that regionally and locally calibrated inversion models can effectively address the problems introduced by spatial heterogeneity in water quality and bottom type, and provide significantly improved bathymetric estimates for more complex coastal waters.

More recently, Eugenio et al. [126] presented an optimal atmospheric correction model, as well as an improved algorithm for sunglint removal based on combined physical and image-processing techniques. The spectral capabilities of World View-2 multispectral imagery (for Granadilla in Tenerife Island and Corralejo in Fuerteventura Island) was exploited for bathymetry retrieval. Using the radiative model to compute bathymetry has yielded good results and allowed to improve the outcome of the ratio algorithm as it considers the physical phenomena of water absorption and backscattering and the relationship between the seafloor albedo, its depth, and the water IOPs. The accuracy of the proposed bathymetry retrieval algorithm output for each coastal area image was assessed with a scatter plot of the algorithm output versus acoustic field data.

In the recent years, several methods based in inversion algorithms and radiative models have been proposed in the literature for retrieving bottom depth from optical remote-sensing imagery. Other approaches have also been tested mainly based in statistical methods. The use of high-resolution optical images seems to improve the accuracy of depth estimation. However, several problems related to atmospheric conditions, SNR, and seafloor contributions are yet to be resolved. There is still a long way to go in using this type of data to estimate the depth for coastal environments through optical remote-sensing data.

5. Conclusions

Different optical satellite data and different methodologies could be used to monitor the coastal environment. There is not an ideal sensor, or an effective technique/algorithm that can be applied to all the coastal environments components/parameters. Depending on what parameter or element is being studied, the selected sensor should have the best characteristics (spatial, spectral, radiometric, and temporal resolution) for the objective proposed. The optimal spatial resolution for the assessment of coastal ecosystems is not consensual. Despite the high spatial resolution images that provide more detail, for several studies low or moderate spatial resolution is enough. Moreover, the low spatial coverage of the high spatial resolution images could be a limiting factor for regional or global studies. The recent developments of hyperspectral sensors that provide very high spectral resolutions introduce a new scenario in this field, allowing, for instance, the development of bio-optical algorithms, more adequate for coastal zones environments. The temporal resolution also depends on the objectives of the research. Various image-processing techniques have been applied to the satellite images in order to study the coastal environment. These techniques differ depending on the subject of study. In the shoreline change detection, beyond visual interpretation, several image segmentation and image classification algorithms are used to identify and detect the evolution of the coastline. Also, several types of algorithms are employed in the quantification of water constituents. A variety of parameters, including Chla, TSM, turbidity, and aCDOM, can be estimated. For instance, in the estimation of Chla, the 700/670 nm ratio reflectance (for high-biomass waters) has been widely used. Alternatively, more complex algorithms, such as ANN, can be employed. Many TSM models are based on empirical methods. However, other algorithms, such as ANN, can also be applied to retrieve the TSM concentration. The identification and monitoring of river plumes can be done considering the water constituents (TSM, salinity, Chla) or applying segmentation and classification algorithms that allow identification of the plume boundaries. The detection and monitoring of HABs require algorithms that have been developed mostly based on extensive in situ bio-optical observations from optically less complex oceanic waters and optical modeling of water properties. Remote-sensing bio-optical algorithms explore the optical properties of each water component. A number of techniques have also been developed for mapping wetlands hazards/vulnerability. When LULC is required, different image classification algorithms can be used. Other algorithms, such PCA, DT, and ANN, can also be used, for instance, in the identification of beach patterns. In the bathymetric estimation, beyond the inversion algorithms and radiative models widely applied, statistical algorithms, such as PCA and ICA can also be used to estimate the depth for estuarine areas. Several advances were discussed related to the recent availability of data from new sensors and hyperspectral data. In short, the assessment of the Sentinel-2 data will improve coastal environment monitoring programs. The elimination of the degree of uncertainty in some procedures should be a priority. There are available at present, a lot of robust, well-tested algorithms that allow quantification and accurate estimation of several parameters. The major challenge still is to have remote-sensing techniques adopted as a routine tool in assessment of change in the coastal zone. Continuing research is required into the techniques employed for assessing change in the coastal environment.

Author details

Ana C. Teodoro*

Address all correspondence to: amteodor@fc.up.pt

Earth Sciences Institute (ICT) and Department of Geosciences, Environment and Land Planning, Faculty of Sciences, University of Porto, Porto, Portugal

References

[1] Cracknell AP: Remote sensing techniques in estuaries and coastal zones – an update. *Int J Remote Sens*. 1999;20(3):485-496.

[2] Malthus TJ, Mumby PJ: Remote sensing of the coastal zone: an overview and priorities for future research. *Int J Remote Sens*. 2003;24(13):2805-2815.

[3] Klemas V: Remote sensing of emergent and submerged wetlands: an overview. *Int J Remote Sens*. 2013;34(18):6286-6320.

[4] Kerekes JP. Optical sensor technology. In: *The SAGE Handbook of Remote Sensing*. Warner TA, Nelis MD, Foody GM, editors. SAGE Publications; 2009. pp. 95-107.

[5] Mouw CB, Greb S, Aurin D, DiGiacomo P, Lee Z, Twardowski M, Binding C, Hu C, Ma R, Moore T, Moses W, Craig S: Aquatic color radiometry remote sensing of coastal and inland waters: challenges and recommendations for future satellite missions. *Remote Sens Environ*. 2015;160:15-30.

[6] Gonçalves H, Teodoro AC, Almeida H: Identification, characterization and analysis of the Douro River Plume from MERIS data. *IEEE J Select Topics Appl Earth Observ Remote Sens*. 2012;5(5):1553-1563.

[7] Feng L, Hu C, Chen X, Tian L, Chen L: Human induced turbidity changes in Poyang Lake between 2000 and 2010: Observations from MODIS. *J Geophys Res*. 2012;117:C07006.

[8] Palmer SCJ, Kutser T, Hunter PD: Remote sensing of inland waters: Challenges, progress and future directions. *Remote Sens Environ*. 2015;157:1-8.

[9] Davranche A, Lefebvre G, Poulin B: Wetland monitoring using classification trees and SPOT-5 seasonal time series. *Remote Sens Environ*. 2010;114(3):552-562.

[10] Santillan J, Makinano M, Paringit E: Integrated Landsat image analysis and hydrologic modeling to detect impacts of 25-Year land-cover change on surface runoff in a Philippine watershed. *Remote Sens*. 2011;3(6):1067-1087.

[11] Hellweger FL, Schlosser P, Lall U, Weissel JK: Use of satellite imagery for water quality studies in New York Harbor. *Estuar Coast Shelf Sci*. 2004;61(3):437-448.

[12] Teodoro AC, Marçal ARS, Veloso-Gomes F: Correlation analysis of water wave reflectance and local TSM concentrations in the breaking zone, using remote sensing techniques. *J Coast Res*. 2007;23(6):1491-1497.

[13] Teodoro AC, Veloso-Gomes F, Goncalves H: Retrieving TSM concentration from multispectral satellite data by multiple regression and artificial neural networks. *IEEE Trans Geosci Remote Sens*. 2007;45(5):1342-1350.

[14] Teodoro AC, Veloso-Gomes F: Quantification of the Total Suspended Matter concentration around the sea breaking zone from in situ measurements and TERRA/ASTER data. *Mar Geores Geotechnol*. 2007;25(2):67-80.

[15] Ouillon S, Douillet P, Petrenko A: Optical algorithms at satellite wavelengths for total suspended matter in tropical coastal waters. *Sensors*. 2008;8:4165-4185.

[16] Ruelland D, Dezetter A, Puech C, Ardoin-Bardin S: Long-term monitoring of land cover changes based on Landsat imagery to improve hydrological modelling in West Africa. *Int J Remote Sens*. 2008;29(12):3533-3551.

[17] Drusch M, Del Bello U, Carlier S, Colin O, Fernandez V, Gascon F, Hoersch B, Isola C, Laberinti P, Martimort P, Meygret A, Spoto F, Sy O, Marchese F, Bargellini P: Sentinel-2: ESA's optical high-resolution mission for GMES operational services. *Remote Sens Environ*. 2012;120:25-36.

[18] Vitousek PM, Mooney HA, Lubchenco J, Melillo JM: Human domination of earth's ecosystems. Science. 1997;277(5325):494-499.

[19] IPCC, 2007: Climate Change 2007: Impacts, Adaptation and Vulnerability. Contribution of Working Group II to the Fourth Assessment Report of the Intergovernmental Panel on Climate Change, M.L. Parry, O.F. Canziani, J.P. Palutikof, P.J. van der Linden and C.E.

[20] Hanson, Eds., Cambridge University Press, Cambridge, UK, 976pp.

[21] Dolan R, Fenster MS, Holme SJ: Temporal analysis of shoreline recession and accretion. *J Coastal Res*. 1991; 7:723-744.

[22] Boak EH, Turner IL: Shoreline definition and detection: a review. *J Coastal Res*. 2005; 21:688-703.

[23] Gens R: Remote sensing of coastlines: detection, extraction and monitoring. *Int J Remote Sens*. 2010;31(7): 1819-1836.

[24] Guariglia A, Buonamassa A, Losurdo A, Saladino R, Trivigno ML, Zaccagnino A, Colangelo A: A multisource approach for coastline mapping and identification of shoreline changes. *Ann Geophys*. 2006;49:295-304.

[25] Ekercin S: Coastline change assessment at the Aegean Sea Coasts in Turkey using multitemporal Landsat imagery. *J Coastal Res*. 2007;23(3):691-698.

[26] Maiti S, Bhattacharya AK: Shoreline change analysis and its application to prediction: A remote sensing and statistics based approach. *Mar Geol*. 2009; 257:11-23.

[27] Kuleli T, Guneroglu A, Karsli F, Dihkan M: Automatic detection of shoreline change on coastal Ramsar wetlands of Turkey. *Ocean Engin*. 2011;38:1141-1149.

[28] Kumar TS, Mahendra RS, Nayak S, Radhakrishnan K, Sahu KC: Coastal vulnerability assessment for Orissa State, East Coast of India. *J Coastal Res*. 2010;26(3):523-534.

[29] Wang CY, Zhang J, Ma Y: Coastline interpretation from multispectral remote sensing images using an association rule algorithm. *Int J Remote Sens*. 2010;31(24):6409-6423.

[30] Teodoro AC, Gonçalves H: A semi-automatic approach for the extraction of sandy bodies (sand spits) from IKONOS-2 data. *IEEE J Select Topics Appl Earth Observ Remote Sens*. 2012;5(2):634-642.

[31] Pardo-Pascual JE, Almonacid-Caballer J, Ruiz LA, Palomar-Vázquez J: Automatic extraction of shorelines from Landsat TM and ETM+ multi-temporal images with subpixel precision. *Remote Sens Environ*. 2012;123:1-11.

[32] García-Rubio G., Huntley D, Russell P: Evaluating shoreline identification using optical satellite images. *Mar Geol*. 2015;359:96-105.

[33] Myint SW, Walker ND: Quantification of surface suspended sediments along a river dominated coast with NOAA AVHRR and SeaWiFS measurements: Louisiana, USA. *Int J Remote Sens*. 2002;23(16):3229-3249.

[34] Matthews MW: A current review of empirical procedures of remote sensing in inland and near-coastal transitional waters. *Int J Remote Sens*. 2011;32(21):6855-6899.

[35] Moses WJ, Gitelson AA, Berdnikov S, Povazhnyy V: Estimation of chlorophyll-a concentration in case II waters using MODIS and MERIS data – successes and challenges. *Environ Res Lett*. 2009;4:045005.

[36] Kiefer I, Odermatt D, Anneville O, Wuest A, Bouffard D: Application of remote sensing for the optimization of in-situ sampling for monitoring of phytoplankton abundance in a large lake. *Sci Total Environ*. 2015;527:493-506 2015.

[37] Gitelson AA, Gurli D, Moses WJ, Barrow, T: A bio-optical algorithm for the remote estimation of the chlorophyll-a concentration in case 2 waters. *Environ Res Lett*. 2009;4:045003.

[38] Le C, Li Y, Zha Y, Sun D, Huang C, Lu H: A four-band semi-analytical model for estimating chlorophyll a in highly turbid lakes: the case of Taihu Lake, China. *Remote Sens Environ*. 2009;113:1175-1182.

[39] Gitelson A, Mayo M, Yacobi YZ, Parparov A, Berman T: The use of highspectral- resolution radiometer data for detection of low chlorophyll concentrations in Lake Kinneret. *J Plankton Res*. 1994;16:993-1002.

[40] Ye HB, Chen CQ, Sun ZH, Tang SL, Song XY, Yang CY, Tian LQ, Liu, FF: Estimation of the primary productivity in Pearl River Estuary using MODIS data. *Estuaries Coasts*. 2015;38(2):506-518.

[41] Giardino C, Candiani G, Zilioli E: Detecting chlorophyll-a in Lake Garda using TOA MERIS radiances. *Photogram Engin Remote Sens*. 2005;71:1045-1051.

[42] Duan HT, Zhang YZ, Zhan B, Song KS, Wang ZM: Assessment of chlorophyll-a concentration and trophic state for Lake Chagan using Landsat TM and field spectral data. *Environ Monitor Assess*. 2007;129(1-3):295-308.

[43] Su YF, et al: A multivariate model for coastal water quality mapping using satellite remote sensing images. *Sensors*. 2008;8(10):6321-6339.

[44] Ormeci C, Sertel E, Sarikaya O: Determination of chlorophyll-a amount in Golden Horn, Istanbul, Turkey using IKONOS and in situ data. *Environ Monitor Assess*. 2009;155(1-4):83-90.

[45] Wu M, Zhang W, Wang X, Luo D: Application of MODIS satellite data in monitoring water quality parameters of Chaohu Lake in China. *Environ Monitor Assess*. 2009;148:255-264.

[46] Tyler AN, Svab E, Preston T, Presing M, Kovacs WA: Remote sensing of the water quality of shallow lakes: A mixture modelling approach to quantifying phytoplankton in water characterized by high-suspended sediment. *Int J Remote Sens*. 2006;27(8): 1521-1537.

[47] Oyama Y, Matsushita B, Fukushima T, Matsushige K, Imai A: Application of spectral decomposition algorithm for mapping water quality in a turbid lake (Lake Kasumigaura, Japan) from Landsat TM data. *ISPRS J Photogram Remote Sens*. 2009;64:73-85.

[48] Doeffer R, Fischer J, Stössel M, Brockman C: Analysis of Thematic Mapper data for studying the suspended matter distribution in the coastal area of the German bight (North Sea). *Remote Sens Environ*. 1989;28:61-73.

[49] Nechad B, Ruddick KG, Park Y: Calibration and validation of a generic multisensor algorithm for mapping of total suspended matter in turbid waters. *Remote Sens Environ*. 2010;114:854-866.

[50] Kong, JL et al.: A semi-analytical model for remote sensing retrieval of suspended sediment concentration in the Gulf of Bohai, China. *Remote Sens*. 2015;7(5):5373-5397.

[51] Kutser T, Arst H, Mäekivi S, Kallaste, K: Estimation of the water quality of the Baltic Sea and lakes in Estonia and Finland by passive optical remote sensing measurements on board vessel. *Lakes Reserv: Res Manag*. 1998;3:53-66.

[52] Bowers D, Harker G, Smith P, Tett, P: Optical properties of a region of freshwater influence (the Clyde Sea). *Estuarine Coastal Shelf Sci*. 2000;50:717-726.

[53] Doxaran D, Cherukuru R, Lavender S: Use of reflectance band ratios to estimate suspended and dissolved matter concentrations in estuarine waters. *Int JRemote Sens*. 2005;26:1763-1770.

[54] D'sa EJ, Miller RL: Bio-optical properties in waters influenced by the Mississippi River during low flow conditions. *Remote Sens Environ*. 2003;84:538-549.

[55] Koponen S, Attila J, Pulliainen J, Kallio K, Pyhälahti T, Lindfors A, Rasmus K, Hallikainen M: A case study of airborne and satellite remote sensing of a spring bloom event in the Gulf of Finland. *Continental Shelf Res*. 2007;27:228-244.

[56] Kutser T, Paavel B, Metsamaa L: Mapping coloured dissolved organic matter concentration in coastal waters. *Int J Remote Sens*. 2009;30:5843-5849.

[57] Loisel H, Vantrepotte V, Dessailly D, Meriaux X: Assessment of the colored dissolved organic matter in coastal waters from ocean color remote sensing. *Optics Express*. 2014;22(11):13109-13124.

[58] Kirk JTO: Optical water quality: What does it mean and how should we measure it?. *J Water Poll Contr Fed*. 1988;60:194-197.

[59] Sun D, Li Y, Wang Q, Gao J, Lv H, Le C, Huang C: Light scattering properties and their relation to the biogeochemical composition of turbid productive waters: A case study of Lake Taihu. *Appl Optics*. 2009;48:1979-1989.

[60] Gitelson AA, Dall'Olmo G, Moses W, Rundquist DC, Barrow T, Fisher TR, Gurlin D, Holz J: A simple semi-analytical model for remote estimation of chlorophyll-a in turbid waters: Validation. *Remote Sens Environ*. 2008;112(9):3582-3593.

[61] Barnes BB, Hu C, Holekamp KL, Blonski S, Spiering BA, Palandro D, et al. Use of Landsat data to track historical water quality changes in Florida Keys marine environments. *Remote Sens Environ*. 2014;140: 485-496.

[62] Hommersom A, Wernand MR, Peters S, de Boer J: A review on substances and processes relevant for optical remote sensing of extremely turbid marine areas, with a focus on the Wadden Sea. *Helgol Mar Res*. 2010;64:75-92.

[63] Dekker AG, Vos RJ, Peters SWM: Comparison of remote sensing data, model results and in situ data for total suspended matter (TSM) in the southern Frisian lakes. *Sci Total Environ*. 2001;268:197-214.

[64] Kaufman, YJ: Solution of the equation of radiative-transfer for remote-sensing over nonuniform surface reflectivity. *J Geophys Res – Oceans Atmos*. 1982;87(NC6): 4137-4147.

[65] Vermote EF, et al.: Second simulation of the satellite signal in the solar spectrum, 6S: An overview. *IEEE Trans Geosci Remote Sens*. 1997;35(3):675-686.

[66] Defoin-Platel M, Chami M: How ambiguous is the inverse problem of ocean color in coastal waters? *J Geophys Res*. 2007;112:C03004.1-C03004.16.

[67] Mélin F, Vantrepotte V: How optically diverse is the coastal ocean? *Remote Sens Environ*. 2015;160:235-251.

[68] Mertes LAK, Warrick JA: Measuring flood output from 110 coastal watersheds in California with field measurements and SeaWiFS. *Geology*. 2001;29:659-662.

[69] Otero P, Ruiz-Villarreal M, Peliz A: River plume fronts off NW Iberia from satellite observations and model data. *ICES J Mar Sci: J du Conseil*. 2009;66(9):1853-1864.

[70] Son YB, Gardner WD, Richardson MJ, Ishizaka J, Ryu JH, Kim SH, Lee SH:Tracing offshore low-salinity plumes in the Northeastern Gulf of Mexico during the summer season by use of multispectral remote-sensing. *J Oceanography*. 2012;68(5):743-760.

[71] Fernández-Nóvoa D, Mendes R, deCastro M, Dias JM, Sánchez-Arcilla A, Gómez-Gesteira M: Analysis of the influence of river discharge and wind on the Ebro turbid plume using MODIS-Aqua and MODIS-Terra data. *J Mar Sys*. 2015;142:40–46.

[72] Teodoro AC, Gonçalves H, Veloso-Gomes F, Gonçalves JA: Modelling of the Douro river plume size, obtained through image segmentation of MERIS data. *IEEE Geosci Remote Sens Lett*. 2009;6(1):87-91.

[73] Jiang L, Yan XH, Klemas V: Remote sensing for the identification of coastal plumes: case studies of Delaware Bay. *Int J Remote Sens*. 2009;30(8):2033-2048.

[74] Guneroglu A, Karsli F, Dihkan M: Automatic detection of coastal plumes using Landsat TM/ETM plus images. *Int J Remote Sens*. 2013;34(13):4702-4714.

[75] Zhu WN, Yu Q: Inversion of chromophoric dissolved organic matter (CDOM) from EO-1 Hyperion imagery for turbid estuarine and coastal waters. *IEEE Trans Geosci Remote Sens*. 2013;51(6): 3286-3298.

[76] Lihan T, Saitoh S, Lida T, Hirawake T, Lida K: Satellite-measured temporal and spatial variability of the Tokachi River plume. *Estuarine Coastal Shelf Sci*. 2008;78:237-249.

[77] Dzwonkowski B, Yan X: Tracking of a Chesapeake Bay estuarine outflow plume with satellite-based ocean color data. *Continental Shelf Res*. 2005;25:1942-1958.

[78] Kim HC, et al.: Distribution of Changjiang diluted water detected by satellite chlorophyll-a and its inter-annual variation during 1998–2007. *J Oceanography*. 2009;65:129-135.

[79] Hopkins J, Lucas M, Dufau C, Sutton M, Stum J, Lauret O, Channelliere C: Detection and variability of the Congo River plume from satellite derived sea surface temperature, salinity, ocean colour and sea level. *Remote Sens Environ*. 2015;139:365-385.

[80] Yonge CM. *The Biology of Reef Building Corals*. London: British Museum, 1940. 353 p.

[81] Smith VE, Rogers RH, Reed LE: Automated mapping and inventory of Great Barrier Reef zonation with Landsat. *Oceans*. 1975;7:775-780.

[82] Kutser T, Miller I, Jupp D: Mapping coral reef benthic substrates using hyperspectral space-borne images and spectral libraries. *Estuarine Coastal Shelf Sci*. 2006;70:449-460.

[83] Purkis SJ: A “Reef-Up” approach to classifying coral habitats from IKONOS imagery. *IEEE Trans Geosci Remote Sens*. 2005;43:1375-1390.

[84] Mishra D, Narumalani S, Rundquist D, Lawson M: Benthic habitat mapping in tropical marine environments using QuickBird multispectral data. *Photogram Engin Remote Sens*. 2006;72:1037-1048.

[85] Mumby PJ, Skirving W, Strong AE, Hardy JT, LeDrew EF, Hochberg EJ, Stumpf RP, David LT: Remote sensing of coral reefs and their physical environment. *Mar Poll Bull*. 2004;48(3-4):219-228.

[86] Kutser T, Dekker AG, Skirving W: Modeling spectral discrimination of Great Barrier Reef benthic communities by remote sensing instruments. *Limnol Oceanography*. 2003;48:497-510.

[87] Knudby A, LeDrew E, Newman C: Progress in the use of remote sensing for coral reef biodiversity studies. *Progr Phys Geography*. 2007;31(4):421-434.

[88] Andréfouët S, Cabioch G, Flamand B, Pelletier B: A reappraisal of the diversity of geomorphological and genetic processes of New Caledonian coral reefs: a synthesis from optical remote sensing, coring and acoustic multibeam observations. *Coral Reefs*. 2009;28(3):691-707.

[89] Hamel MA, Andréfouët S: Using very high resolution remote sensing for the management of coral reef fisheries: Review and perspectives. *Mar Poll Bull*. 2010;60(9): 1397-1405.

[90] Palandro DA, Andrefouet S, Hu C, Hallock P, Muller-Karger FE, Dustan P, Callahan MK, Kranenburg C, Beaver CR: Quantification of two decades of shallow-water coral reef habitat decline in the Florida Keys National Marine Sanctuary using Landsat data (1984-2002). *Remote Sens Environ*. 2008;112(8):3388-3399.

[91] Ahn YH, Shanmugam P, Ryu JH, Jeong JC: Satellite detection of harmful algal bloom occurrences in Korean waters. *Harmful Algae News*. 2006; 213-131.

[92] Gao X, Song J: Phytoplankton distributions and their relationship with the environment in the Changjiang Estuary, China. *Mar Poll Bull*. 2005;50:327-335.

[93] Tang DL, Kawamura H, Oh IS, Baker J: Satellite evidence of harmful algal blooms and related oceanographic features in the Bohai Sea during autumn 1998. *Adv Space Res*. 2006;37:681-689.

[94] Tomlinson M., Wynne TT, Stumpf RP: An evaluation of remote sensing techniques for enhanced detection of the toxic dinoflagellate, Karenia brevis. *Remote Sens Environ*. 2009;113:598-609.

[95] Klemas V: Remote sensing of algal blooms: An overview with case studies. *J Coastal Res*. 2012;28(1A):34-43.

[96] Mahendra RS, Mohanty PC, Bisoyi H, Srinivas T, Kumar, Nayak, S: Assessment and management of coastal multi-hazard vulnerability along the Cuddalore Villupuram, east coast of India using geospatial techniques. *Ocean Coastal Manag*. 2011;54: 302-311.

[97] Gilmore MS, Wilson EH, Barrett N, Civco DL, Prisloe S, Hurd JD, Chadwick C: Integrating multitemporal spectral and structural information to map wetland vegetation in a Lower Connecticut River Tidal Marsh. *Remote Sens Environ*. 2008;112:4048-4060.

[98] Cavalli RM, Laneve L, Fusilli S, Pignatti F, Santini: Remote sensing water observation for supporting Lake Victoria weed management. *J Environ Manag*. 2009;90(7): 2199-2211.

[99] Klemas V: Remote sensing of wetlands: Case studies comparing practical techniques. *J Coastal Res*. 2011;27: 418-427.

[100] Li M, L Zhong WC, Boicourt S, Zhang, Zhang D: Hurricane-induced stratification and destratification in a partially-mixed estuary. *J Mar Res*. 2007;65:169-192.

[101] Laba M, Downs R, Smith S, Welsh S, Neider C, White S, Richmond M, Philpot W, Baveye P: Mapping invasive wetland plants in the Hudson River National Estuarine Research Reserve using Quickbird satellite imagery. *Remote Sens Environ*. 2008;112: 286-300.

[102] Hirano A, Madden M, Welch R: Hyperspectral image data for mapping wetland vegetation. *Wetlands*. 2003;23:436-448.

[103] Yang X. *Remote Sensing and Geospatial Technologies for Coastal Ecosystem Assessment and Management*. Berlin: Springer-Verlag; 2009.

[104] Heumann BW: Satellite remote sensing of mangrove forests: Recent advances and future opportunities. *Progr Phys Geography*. 2011;35:87-108.

[105] Baker C, Lawrence RL, Montagne C, Patten D: Change detection of wetland ecosystems using Landsat imagery and change vector analysis. *Wetlands*. 2007;27:610-619.

[106] Ramsey E, Rangoonwala A. Mapping the onset and progression of marsh dieback. In: *Remote Sensing of Coastal Environment*, J. Wang, editor. Boca Raton, FL: CRC Press; 2010. pp. 123-150.

[107] Fan F, Wang Y, Wang Z: Temporal and spatial change detecting (1998–2003) and predicting of land use and land cover in Core corridor of Pearl River Delta (China) by using TM and ETM+ images. *Environ Monitoring Assess*. 2008;137:127-147.

[108] Abd El-Kawy OR, Rød JK, Ismail HA, Suliman AS: Land use and land cover change detection in the western Nile delta of Egypt using remote sensing data. *Appl Geography*. 2011;31:483-494.

[109] Tran H, Tran T, Kervyn M: Dynamics of land cover/land use changes in the Mekong Delta, 1973-2011: A remote sensing analysis of the Tran Van Thoi District, Ca Mau Province, Vietnam. *Remote Sens*. 2015;7:2899-2925.

[110] Kumpulainen S. Vulnerability concepts in hazard and risk assessment. Natural and technological hazards and risks affecting the spatial development of European re-

gions. In: Schmidt-Thomé, Philipp, editors. Geological Survey of Finland, Special Paper 42: 2006. pp. 65-74.

[111] Römer H, Willroth P, Kaiser G, Vafeidis AT, Ludwig R, Sterr H, Revilla Diez J: Potential of remote sensing techniques for tsunami hazard and vulnerability analysis – a case study from Phang-Nga province, Thailand. *Natur Haz Earth Sys Sci*. 2012;12:2103-2126.

[112] Teodoro AC, Pais-Barbosa J, Veloso-Gomes F, Taveira-Pinto F: Evaluation of beach hydromorphological behaviour and classification using image classification techniques. *J Coastal Res*. 2009;2(56):1607-1611.

[113] Teodoro AC, Pais-Barbosa J, Gonçalves H, Veloso-Gomes F, Taveira-Pinto F: Identification of beach features/patterns through image classification techniques applied to remotely sensed data. *Int J Remote Sens*. 2011;32(22):7399-7422.

[114] Teodoro AC: Applicability of data mining algorithms in the identification of beach features/patterns on high-resolution satellite data. *J Appl Remote Sens*. 2015;9(1): 095095.

[115] Lyzenga DR, Malinas N P, Tanis F J: Multispectral bathymetry using a simple physically based algorithm. *IEEE Trans Geosci Remote Sens*. 2006;44(8):2251-2259.

[116] Kanno A, Koibuchi Y, Isobe M: Statistical combination of spatial interpolation and multispectral remote sensing for shallow water bathymetry. *IEEE Geosci Remote Sens Lett*. 2011;8(1)64-67.

[117] Teodoro AC, Almeida R, Gonçalves M: Independent Component Analysis (ICA) performance to bathymetric estimation using high resolution satellite data in an estuarine environment, in Remote Sensing for Agriculture, Ecosystems, and Hydrology XVI, Christopher M. U. Neale; Antonino Maltese, Editors, Proceedings of SPIE Vol. 9239 (SPIE, Bellingham, WA 2014), 923915.

[118] Su H, Liu H, Wang L, Filippi AM, Heyman WD, Beck RA: Geographically adaptive inversion model for improving bathymetric retrieval from satellite multispectral imagery. IEEE Trans Geosci Remote Sens. 2014;52(1): 465-476.

[119] Lesser MP, Mobley CD: Bathymetry, water optical properties, and benthic classification of coral reefs using hyperspectral remote sensing imagery. *Coral Reefs*. 2007;26(4):819-829.

[120] Su H, Liu H, Heyman W: Automated derivation of bathymetric information from multispectral satellite imagery using a nonlinear inversion model. *Mar Geodesy*. 2008;31(4):281-298.

[121] Lyzenga DR: Passive remote sensing techniques for mapping water depth and bottom features. *Appl Optics*. 1978;17:379-383.

[122] Lyzenga DR: Remote sensing of bottom reflectance and water attenuation parameters in shallow water using aircraft and Landsat data. Int J Remote Sens. 1981;2(1): 71-82.

[123] Lyzenga DR: Shallow-water bathymetry using combined lidar and passive multispectral scanner data. Int J Remote Sens. 1985;6(1):115-125.

[124] Minghelli-Roman A, Goreac A, Mathieu, S, Spigai M, Gouton P: Comparison of bathymetric estimation using different satellite images in coastal sea waters. Int J Remote Sens. 2009;30(21):5737-5750.

[125] Teodoro AC, Gonçalves H, Pais-Barbosa J: Bathymetric estimation through principal components analysis using IKONOS-2 data, in Remote Sensing for Agriculture, Ecosystems, and Hydrology XII, Christopher M. U. Neale; Antonino Maltese, Editors, Proceedings of SPIE Vol. 7824 (SPIE, Bellingham, WA 2010), 782419.

[126] Eugenio F, Marcello J, Javier Martin J: High-resolution maps of bathymetry and benthic habitats in shallow-water environments using multispectral remote sensing imagery. IEEE Trans Geosci Remote Sens. 2015;53(7):3539-3549.